

Exploring Modal Switch in Metamaterial-Based Robots

Britton Jordan¹, Daniel S. Esser², Jeonghyeon Kim¹, Brian Y. Cho¹, Robert J. Webster III², and Alan Kuntz¹

Abstract—Mechanical metamaterials are microscale patterned structures that are designed to have specific mechanical properties at a macro-scale that are atypical of natural materials. Robotic manipulators composed of these materials can exhibit deformation and motion capabilities that can be customized and easily fabricated. However, as of now, the motion capability of such manipulators are encoded in their physical composition and cannot be changed. This paper presents multi-modal metamaterial-based robot prototypes which can switch between the behaviors found in two different metamaterials. Two such robots are explored, a bending/shearing robot and a bending/twisting robot. The robot design is described in detail, including how the robots toggle between behavior modes via mechanical actuation of a sliding rod insert. Multi-modal robots are compared to their single-mode equivalents to characterize their capabilities. The single-mode behaviors are largely preserved in the multi-modal innovations. The multi-modal prototypes also demonstrate variable rigidity. We discuss the feasibility of using robots of this design as part of a robotic surgical system.

I. INTRODUCTION

Metamaterials consist of micro-patterned structures of constituent materials that, when manipulated at the macro-scale, result in customized mechanical properties typically not found in homogeneous materials. These composite structures can be realized via additive manufacturing of flexible and rigid elements to enable complex motion of the entire structure with specific applied forces at one location [1], [2]. As an example, with a specific 3D printed geometry, a long structure can be made that bends or shears along its length when only one end of the structure is mechanically compressed (see Fig. 1 top).

In the literature, there are different classes of metamaterials that result in macro-scale deformation properties that homogeneous materials cannot achieve. Pentamode metamaterials can flow like liquids and conform around rigid objects due to a much larger bulk modulus (stiffness to uniform forces) compared to their shear modulus [3], [4]. Near zero or even negative stiffness can be achieved with bistable structures that can snap between two stable configurations

¹Britton Jordan, Jeonghyeon Kim, Brian Y. Cho, and Alan Kuntz are with the Robotics Center and the Kahlert School of Computing at the University of Utah, Salt Lake City, UT 84112, USA; (email: alan.kuntz@utah.edu).

²Daniel S. Esser and Robert J. Webster III are with the Department of Mechanical Engineering, Vanderbilt University, Nashville, TN, 37203.

This material is based upon work supported in part by the National Science Foundation under grant number 2133027. Any opinions, findings, and conclusions or recommendations expressed in this material are those of the authors and do not necessarily reflect the views of the NSF. B. Jordan was also supported in part by the Undergraduate Research Opportunity Program at the University of Utah, and D. Esser was partially supported by the Natural Sciences and Engineering Research Council of Canada (NSERC) under grant 521537544.

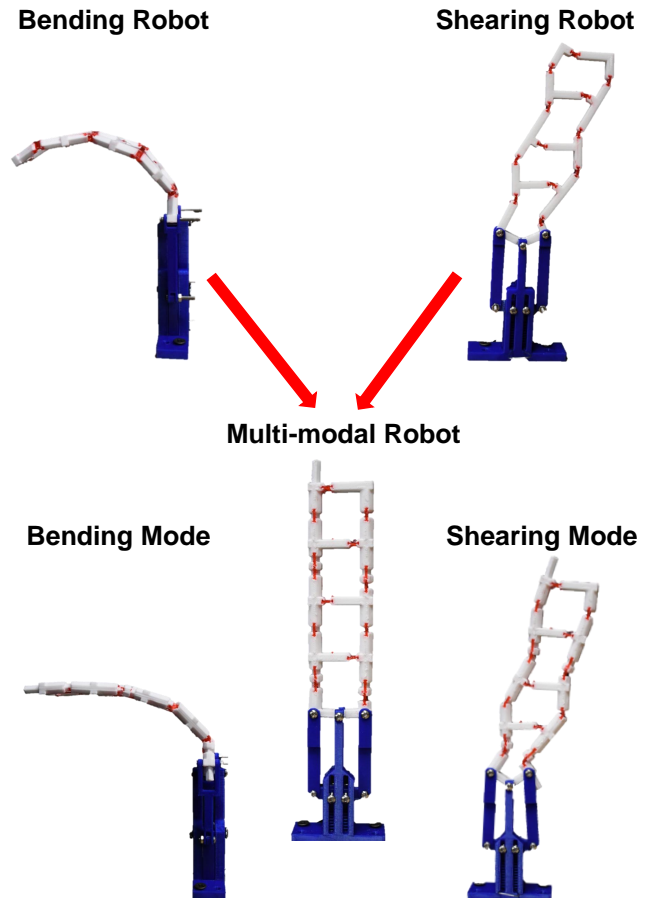


Fig. 1: In this work, the mechanical properties of two separate metamaterial robots are combined to create a multi-modal innovation which exhibits both behaviors in a single design.

and store/release energy during these transitions [5], [6]. Of particular interest in the soft robotics community, auxetic metamaterials demonstrate a negative Poisson ratio; as they are extended, they grow wider rather than narrowing [7]–[9].

Due to the uniquely high tunability of mechanical metamaterials, robotic manipulators composed of such materials can be designed to best suit very specific task requirements. A desired complex motion can be achieved where only a simple actuation input is required [10], [11]. This is similar to some continuum robotics research, in which robots have also been preprogrammed to satisfy task requirements. For example, multi-backbone tendon robots have been proposed to change the bending stiffness to shift the workspace of the continuum robot [12].

Such design approaches work well for specific, unchang-

ing tasks. However, since the behavior of these structures must be mechanically encoded in their design, once manufactured the deformation characteristics are fixed [13]. For example, the two mechanical metamaterial designs shown in Fig. 1, top, are each only capable of one mode of deformation. The left design bends when its base is compressed and the right design exhibits a shearing motion when its base is compressed. However, each of these designs, and those like them, can *only* exhibit a single, preprogrammed motion when actuated. This severely limits the potential for the use of these types of structures in a general-purpose robotic manipulator, as robot behavior must change as task requirements change.

Advancements have been made to add post-fabrication tunability to robots with task-fitting preprogrammed structures, mostly with regard to variable stiffness. Particle or layer jamming techniques force material to a concentrated location of a soft robot to create a more stiff segment [14]. Another innovation toggles from a stiff to a soft mode by mechanically separating a rigid backbone [15]. Magnetic locking mechanisms have been proposed to lock continuum segments in place [16]. Thermally responsive materials [17]–[19] and shape-memory alloys [20] have been used to control the bending stiffness parameters during a robotic task. Other structures composed of gears or cams are capable of transforming continuously through a range of stiffnesses [21].

In contrast with prior examples of variable stiffness mechanisms which typically focus on changing the amount or direction of bending, our proposed designs are capable of changing between two different deformation modes. We use mechanical metamaterials to create novel, easy-to-fabricate hyper-redundant robots that enable multiple types of deformation modes such as bending, shearing, and twisting, when a uniaxial force is applied to the structure at its base. A simple adjustment of the robot structure switches it between two modes, enabling the deformations of two metamaterials in one robot. The robot is actuated with the same input in each mode. The hinges that enable both deformation modes are housed on two rods that slide within the robot's rigid backbones. Hinges of a single deformation align with gaps in the backbone to activate one mode of behavior at a time. We produce viable prototypes with flexible hinges, demonstrating this concept's appropriateness for robotic applications such as minimally-invasive surgery (MIS), where passive structural compliance is important.

These multi-modal robots are low-cost and easy to fabricate. They retain the task-specific pre-programmability of conventional metamaterials with the added versatility of multiple deformation modes. We envision their use as standalone general-purpose manipulators or as part of a conformable robotic system. Various designs of flexible robots have been developed for surgical applications as their slender, curvilinear nature enables them to bend through narrow anatomical passageways [22]. We have previously proposed additively manufactured millimeter-scale wrists based on tendon actuation [23] to improve the dexterity of microsurgical tools [24], however assembling tendon-driven robots at such a scale is particularly challenging. Because the metamaterial

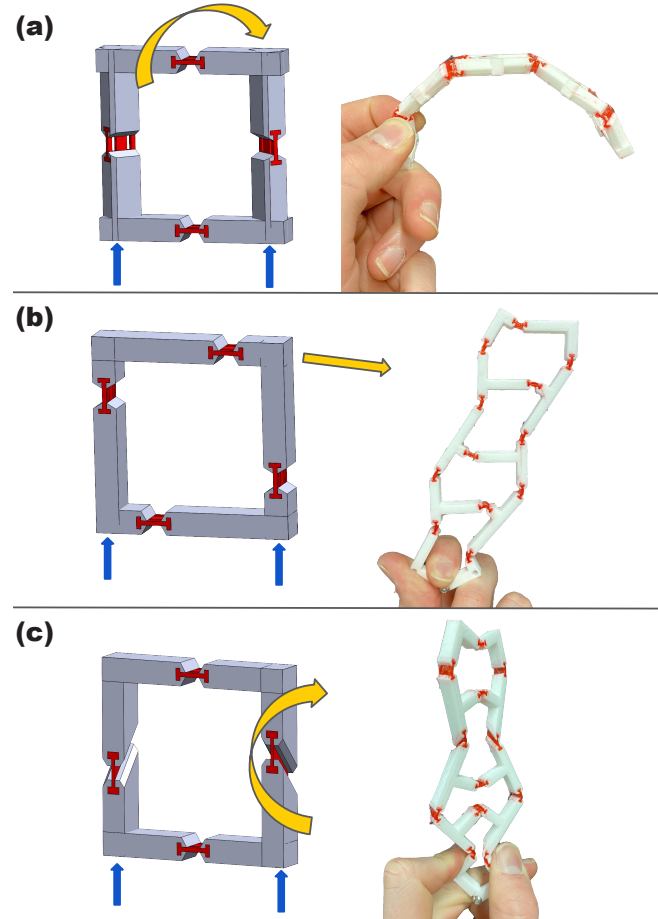


Fig. 2: Three prototypes demonstrating the three single modes of deformation: (a) bending (b) shearing and (c) twisting. Each design is actuated by a planar compressive force on the base links of the robot. The structures contain flexible, narrow joints fabricated with thermoplastic polyurethane (red) that permit rotation about an axis. The orientation of these joints causes the constitutive links (grey/white) of the structure to bend in a prescribed manner.

robots in this work are actuated by applying forces through their structure, they require few parts and minimal assembly, which may make them good candidates for miniaturization.

II. MULTI-MODAL METAMATERIAL ROBOT CONCEPT

A. Single mode behavior

Based on the designs proposed in [2], we fabricate three single-mode manipulators (shown in Fig. 2) as baseline comparisons to our multi-modal designs. We use thin sections of a flexible material to create elastic hinges between thicker rigid links. Each 4×4 cm unit is composed of four rigid links at the corners, connected by joints on each side of the square. Units are tessellated into a line to create a single manipulator. These models were produced using multi-material additive manufacturing from thermoplastic polyurethane (TPU) and polylactic acid (PLA) filaments. We will refer to the plane in which the tessellation occurs as the construction plane.

The bending unit (see (a) of Fig. 2) has joints on the top and bottom oriented along the \hat{z} axis allowing it to extend

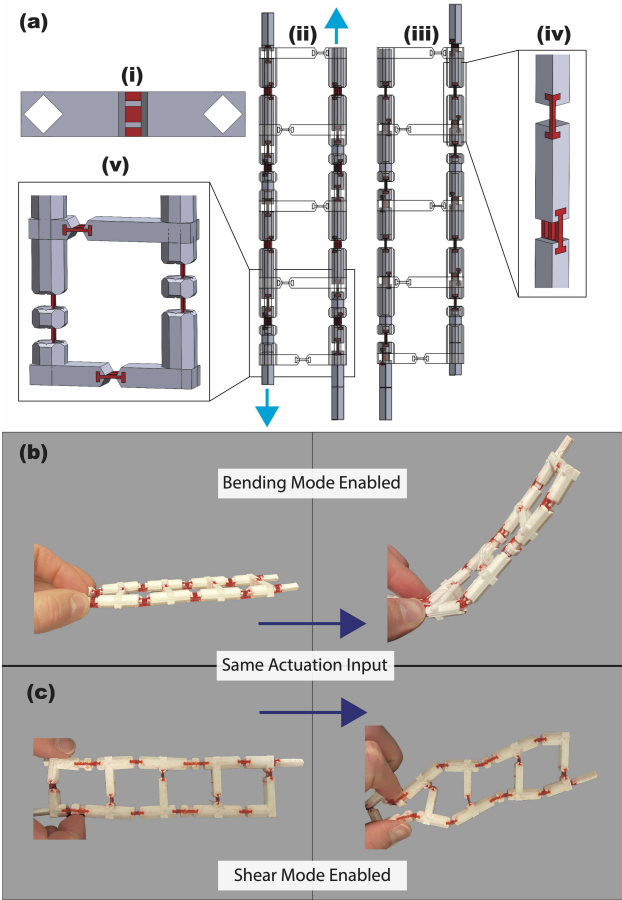


Fig. 3: (a) CAD model for the multi-modal bending/shearing robot. (a.i) View from base (a.ii) Bending configuration with arrows annotating translation of the rods to expose the shearing hinges (a.iii) Shearing configuration (a.iv) Detailed view of the rod (a.v) Detailed view of the base unit of the backbone. (b) Deformation of the prototype when the bending joints are exposed, i.e., bending mode is enabled; and (c) when the shearing mode is enabled.

along the \hat{y} axis. Relative to the top and bottom joints, the joints on the left and right sides are rotated 45° in opposite directions about the \hat{x} axis, such that they bend inwards towards each other and out of the construction plane (about the \hat{x} axis). The shearing unit (see (b) of Fig. 2) is composed of four identical links with joints aligned along the \hat{z} axis, with each joint offset from the center of each side of the square. This results in a net displacement of the top side of the square to the right. The twisting unit (see (c) of Fig. 2) has joints on the top and bottom oriented along the \hat{z} axis similar to the bending unit. Relative to the top and bottom joints, the joints on the left and right sides are rotated 45° in opposite directions about the \hat{y} axis, such that they bend inwards towards each other and generate a net twist about the \hat{x} axis.

When tessellating units, two identical and adjacent units would cause a canceling effect with no net planar transformation. Thus, the shearing and twisting units are connected with units that have symmetric joints (oriented along \hat{z}) on the left and right sides which serve to invert the motion for the next

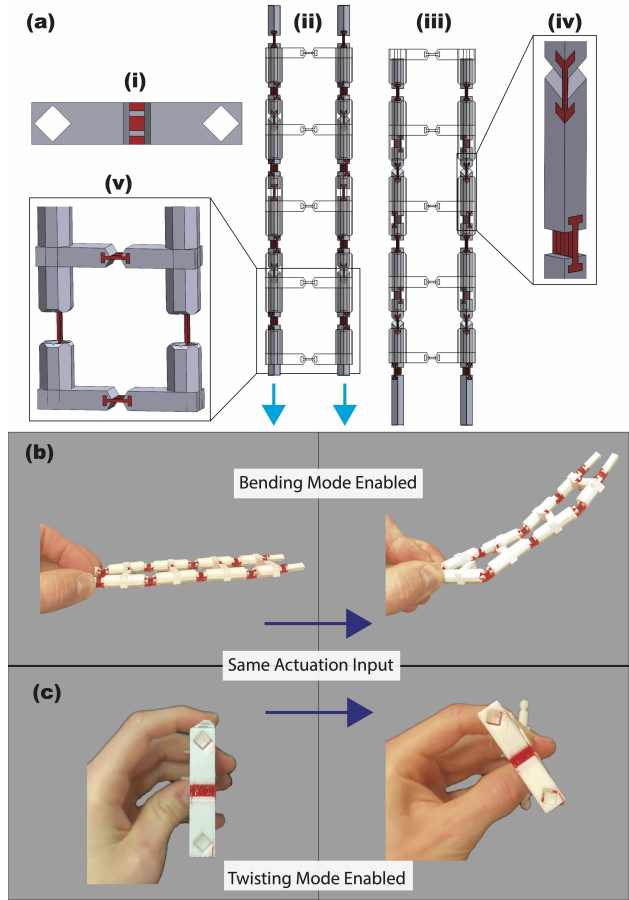


Fig. 4: (a) CAD model for the multi-modal bending/twisting robot. (a.i) View from base (a.ii) Bending configuration with arrows annotating translation of the rods to switch to the twisting mode (a.iii) Twisting configuration (a.iv) Detailed view of the rod (a.v) Detailed view of the base unit of the backbone (b) Prototype behavior in the bending mode and (c) the twisting mode.

unit in the line. For the bending design, the same bending unit rotated 180° out of the construction plane achieves the desired motion inversion.

B. Multi-modal behavior

We propose a novel design that enables a single robot to have the behavior of different metamaterials. The behavior of these robots can be changed between two modes on-demand. We demonstrate two implementations of this concept, a bending/shearing robot and a bending/twisting robot.

To achieve this we design long rods with a square cross-section which are inserted into correspondingly-shaped slots in the rigid robot backbones, one on each side of the robot (see (a.i) of Fig. 3 and 4). Along each rod we strategically place and orient all the hinges needed for each of two metamaterial behaviors. We select which of the two metamaterial behaviors is active by only allowing certain hinges to bend. Hinges are kept from bending by situating them within the cavity of a rigid section of the backbone. Hinges are allowed to bend by situating them in a gap between rigid material sections. The robot backbone is held together by thin flexible connectors, keeping the rigid sections of the backbone the

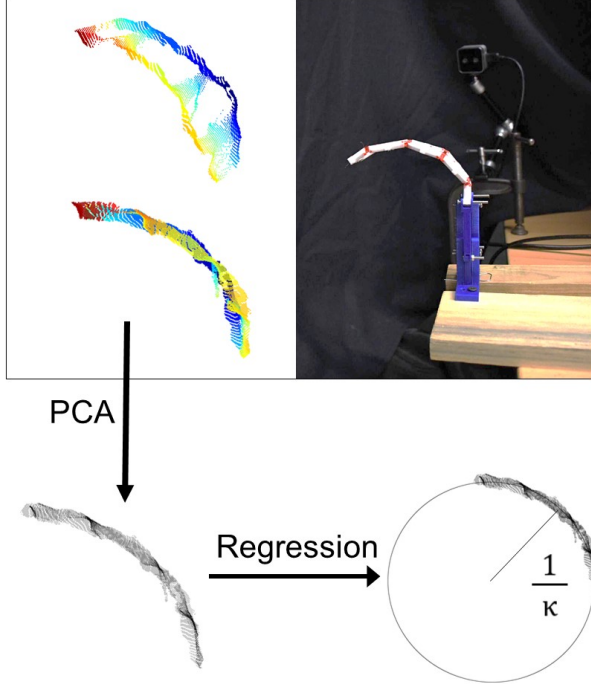


Fig. 5: The measurement process used for characterising the bending behavior. We apply principal component analysis (PCA) to the 3D point cloud to find the bending plane, and then calculate the bending curvature by fitting a circle to the projected points.

appropriate distance apart while allowing them to move freely relative to one another.

We place the hinges from each long edge of a single-mode robot with identical spacing and orientation along the two rod inserts. Then, we do the same with the hinges from a second single-mode robot, placing this arrangement of hinges at a strategic offset from those of the first. This offset distance is the same distance the rod must be translated to toggle between modes. These distances are somewhat arbitrary, but are chosen such that only one arrangement of hinges will align with the gaps in the backbone at a time.

The hinges of the units running across the length of the robot differ between the single-mode bending and single-mode shearing robots. When considering the multi-modal design, switching the hinges found within the units is not possible with the sliding rod concept. We elect to use the alternating offset hinges for these sides because they work well for both modes.

III. CHARACTERIZATION

We characterize the new multi-modal metamaterial robots via experimental comparison to the single mode versions to understand to what extent each single mode behavior is preserved when combined in a multi-modal robot.

We actuate the robots in a consistent, measurable way by using a 3D printed mount. Each robot design is modified to have a centrally located sliding hinge at its base which is fixed to the grounded mount. An unanchored part of the mount has two arms that attach to the robot for actuation, one on each corner of the robot base. The arms move in

tandem such that the robot is actuated with a single degree of freedom. Equally spaced slots in the unanchored part of the mount allow the displacement to be measured. The displacement is fixed at each actuation distance by inserting a pin into the appropriate slot.

We use an RGB-D camera (*Intel: Realsense D405*) to obtain a point cloud of the robot as it is actuated. Using the point cloud we produce an appropriate comparison metric for each behavior, i.e., bending, shearing, and twisting. The experimental setup to actuate the robots and measure the deformed shape is shown in Fig. 5.

For the robots that bend we use the bending curvature as our metric of comparison. We apply principal component analysis (PCA) to the 3D point cloud to determine the plane of bending. We use a least squares regression to fit these projected points to a circle with radius r which is used to calculate curvature using $\kappa = \frac{1}{r}$.

For the shearing behavior, we analyze each actuated point cloud in comparison to the unactuated point cloud to determine the displacement vector of the robot tip.

For the twisting behavior, we use the angle of displacement between the robot's beginning and end segments as our comparison metric. We use PCA to determine the principal axis of the links at the beginning and end segments.

A. Bending comparison

We compare the behavior of the single-mode bending robot to that of the multi-modal robots configured to the bend mode by measuring the curvature as a function of the actuation distance beginning from an unactuated state at 2 mm intervals (see (a) of Fig. 6). Intuitively, the curvature of the robot increases as the actuation distance increases. For the single mode and both multi-modal robots, the curvature increases linearly with the actuation distance. The slope of this relationship is steeper for the single mode robot, reaching a curvature of $16.6 \frac{1}{m}$ when actuated 10 mm. The two multi-modal robots behave similarly to each other. The bending/shearing robot has a curvature of $9.8 \frac{1}{m}$ when actuated 10 mm, while the bending/twisting robot has a curvature of $9.5 \frac{1}{m}$ at this actuation distance.

We see a slightly diminished bend in the multi-modal robots configured to their bending mode compared to the single-mode robot. As the multi-modal robot is actuated, the deformation in each subsequent units decreases towards the tip. This may be attributed to the gap between the rod insert and backbone; this clearance in the slot is required for the rod to slide freely, though as a result the play in the mechanism slightly reducing the intended motion as the robot is actuated.

B. Shearing comparison

We measure the displacement vector of the single-mode shearing robot and multi-modal bending/shearing robot in the shearing mode beginning from an unactuated state at 2 mm intervals (see (b) of Fig. 6). The behavior between the two robots is very similar; the shearing ability is well preserved in the multi-modal robot. In fact, the multi-modal robot sees a slightly greater shearing displacement than the

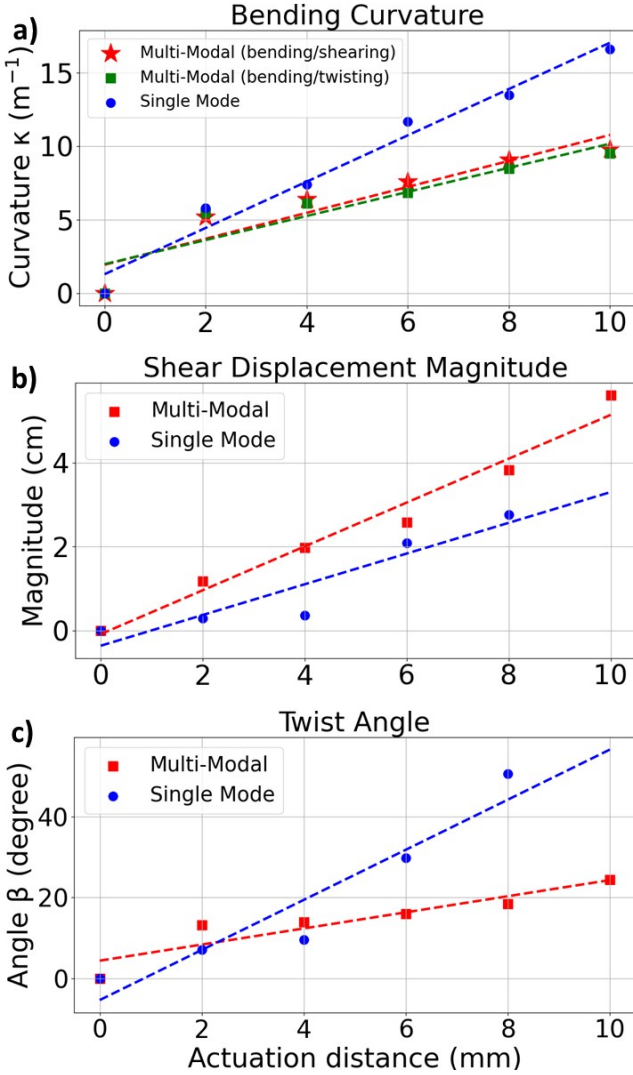


Fig. 6: Plots comparing the behavior of the single mode robots to their multi-modal equivalents. (a) shows the curvature of the single mode bending robot compared to both multi-modal robots in the bending mode. (b) compares the magnitude of displacement between single mode and multi-modal shearing. (c) shows the angle of displacement for the twisting robots.

single mode version. For both robots, approximately 80% of the displacement of the robot tip is in the horizontal direction, with a small displacement in the vertical direction. At an actuation distance of 8 mm the magnitude of the displacement vector is 2.8 cm for the single mode robot and 3.8 cm for the multi-modal robot.

C. Twisting comparison

We measure the twist angle of the single mode twisting robot and multi-modal bending/twisting robot in the twisting mode beginning from an unactuated state at 2 mm intervals (see (c) of Fig. 6). For both robots, the relationship between angle and actuation distance is linear. The single mode robot is capable of a greater twist, reaching an angle of 50.6° at the maximum possible actuation of 8 mm. By contrast, in the multi-modal case, the robot achieves a 18.4° twist when

actuated 8 mm. Similar to the bending multi-modal case, gaps between the rod and backbone allow for movement which inhibits the intended shape, resulting in less twist.

D. Single mode vs. multi-modal supporting load

We perform an experiment to determine how the multi-modal robot compares to the single mode robot in its ability to support a load (see Fig. 7). Orienting the robot parallel to the ground, we measure the displacement of the robot when supporting and not supporting a weight. For this experiment we measure the displacement vector of the robot tip using the same method as the shearing behavior analysis above. We apply 0.2 N at the tip with a calibration weight for the bending behavior and 0.3 N for shearing. The twisting behavior is not measured in this experiment. We repeat the experiment for actuation distances from 0–12 mm in 4 mm increments.

The displacement caused by the weight is similar across all actuation distances. For the single-mode bending robot the average displacement is 1.84 cm, while the multi-modal bending has an average of 5.56 cm. The single-mode shearing robot has an unmeasurably small displacement at all actuation distance, while the multi-modal robot has an average displacement of 0.81 cm.

The multi-modal robots exhibit a larger displacement under load than do the single mode robots. As discussed previously, this could be due in part to the gap between the sliding rods and the backbone. Additionally, the hinges used for the multi-modal robots are significantly smaller in order to accommodate putting them on the rod, providing less resistance to external loading.

E. Variable rigidity with mode change

Through qualitative observation we see how changing between modes affects the rigidity of the multi-modal robot (see Fig. 8). We observe the bending/twisting robot supporting a 0.1 N weight hanging from its tip when configured to each state. We see that the robot has higher passive bending stiffness in the twist configuration. When in the bend configuration, the robot is less stiff but can be actuated to lift the weight. Tuneable stiffness could be a valuable capability in the context of MIS where a manipulator must navigate

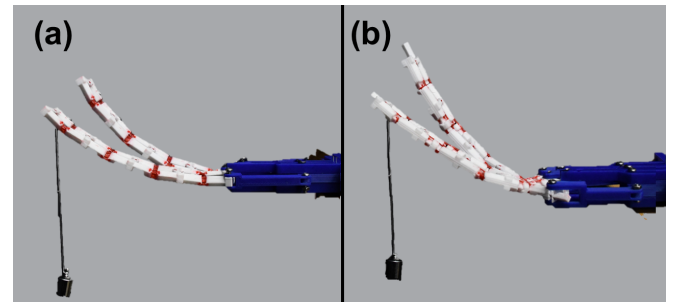


Fig. 7: Rigidity experiment with a 0.2 N weight comparing (a) single mode and (b) multi-modal bending. The displacement of the multi-modal robot when supporting a weight at its tip (b) is greater than that of the single mode robot (a).

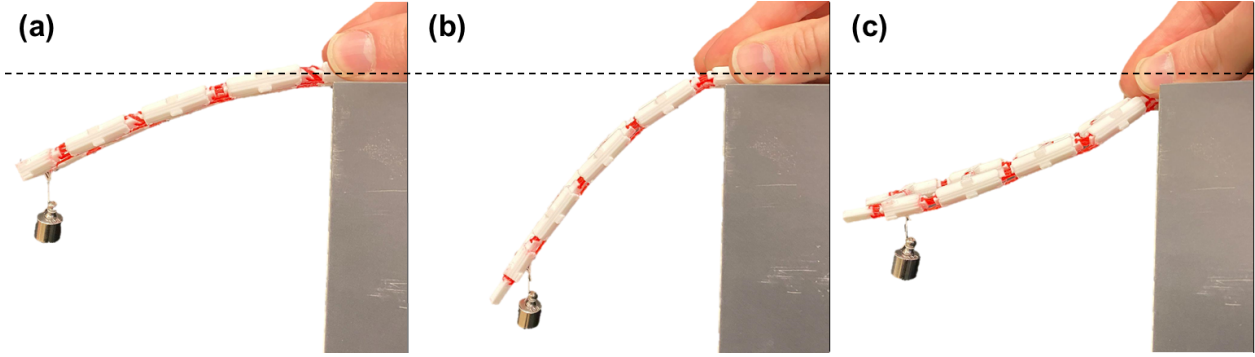


Fig. 8: Rigidity experiment with a 0.1 N weight comparing between modes of the bending/twisting prototype. (a) shows the prototype when it is configured to twist, in which case it has a higher stiffness to out-of-plane loading at the tip. When switched to the bending mode, the stiffness is lower and the tip deflects more (b). However, in this mode, the robot can be actuated to lift this external load (c).

near delicate biological tissue while still being able to apply a force to perform surgical tasks.

IV. CONCLUSION

Overall, the capabilities of the single mode metamaterial robots are preserved in the multi-modal designs. Towards future microsurgical applications, we plan on miniaturizing these devices using alternative fabrication techniques, such as two-photon polymerization or laser tube cutting. We believe that multi-modal metamaterial robots are a promising solution for a dexterous, versatile, and general-purpose tool in surgical and other applications. However, their ability to switch between modes with different stiffness and deformation properties is necessary to realize these applications. Further advancements in this direction could lead to the creation of sophisticated hyper-redundant robotic systems which improve surgery success rates through their enhanced capabilities for precise and controlled manipulation.

REFERENCES

- [1] A. G. Mark, S. Palagi, T. Qiu, and P. Fischer, "Auxetic metamaterial simplifies soft robot design," in *2016 IEEE International Conference on Robotics and Automation (ICRA)*, May 2016, pp. 4951–4956.
- [2] J. Ou, Z. Ma, J. Peters, S. Dai, N. Vlavianos, and H. Ishii, "KinetiX - designing auxetic-inspired deformable material structures," *Computers & Graphics*, vol. 75, pp. 72–81, Oct. 2018.
- [3] T. Bückmann, M. Thiel, M. Kadic, R. Schittny, and M. Wegener, "An elasto-mechanical unfeelability cloak made of pentamode metamaterials," *Nature communications*, vol. 5, no. 1, p. 4130, 2014.
- [4] R. Schittny, T. Bückmann, M. Kadic, and M. Wegener, "Elastic measurements on macroscopic three-dimensional pentamode metamaterials," *Applied physics letters*, vol. 103, no. 23, 2013.
- [5] S. Shan, S. H. Kang, J. R. Raney, P. Wang, L. Fang, F. Candido, J. A. Lewis, and K. Bertoldi, "Multistable Architected Materials for Trapping Elastic Strain Energy," *Advanced materials.*, vol. 27, no. 29, pp. 4296–4301, 2015.
- [6] A. Rafsanjani, A. Akbarzadeh, and D. Pasini, "Snapping Mechanical Metamaterials under Tension," *Advanced materials.*, vol. 27, no. 39, pp. 5931–5935, 2015.
- [7] A. Sedal, M. Fisher, J. Bishop-Moser, A. Wineman, and S. Kota, "Auxetic Sleeves for Soft Actuators with Kinematically Varied Surfaces," in *2018 IEEE/RSJ International Conference on Intelligent Robots and Systems (IROS)*. IEEE, 2018, pp. 464–471.
- [8] P. Kaarthik, F. L. Sanchez, J. Avtges, and R. L. Truby, "Motorized, untethered soft robots 3D printed auxetics," *Soft matter*, vol. 18, no. 43, pp. 8229–8237, 2022.
- [9] Y. Dikici, H. Jiang, B. Li, K. A. Dalorio, and O. Akkus, "Piece-By-Piece Shape-Morphing: Engineering Compatible Auxetic and Non-Auxetic Lattices to Improve Soft Robot Performance in Confined Spaces," *Advanced engineering materials*, vol. 24, no. 9, 2022.
- [10] F. Vanneste, O. Goury, J. Martínez, S. Lefebvre, H. Delingette, and C. Duriez, "Anisotropic soft robots based on 3d printed mesostructured materials: Design, modeling by homogenization and simulation," *IEEE Robotics and Automation Letters*, vol. 5, no. 2, pp. 2380–2386, April 2020.
- [11] A. Rafsanjani, K. Bertoldi, and A. R. Studart, "Programming soft robots with flexible mechanical metamaterials," *Science Robotics*, vol. 4, no. 29, p. eaav7874, 2019.
- [12] J. Barrientos-Diez, M. Russo, X. Dong, D. Axinte, and J. Kell, "Asymmetric Continuum Robots," *IEEE robotics and automation letters*, vol. 8, no. 3, pp. 1279–1286, 2023.
- [13] X. Li, W. Peng, W. Wu, J. Xiong, and Y. Lu, "Auxetic mechanical metamaterials: from soft to stiff," *International Journal of Extreme Manufacturing*, vol. 5, no. 4, p. 042003, Jul. 2023.
- [14] Z. Liu, L. Xu, X. Liang, and J. Liu, "Stiffness-tunable segment for continuum soft robots with vertebrae," *Machines*, vol. 10, no. 7, 2022.
- [15] H. Wang, Z. Zhou, X. Yang, and X. Zhang, "A switchable rigid-continuum robot arm: Design and testing," in *2022 International Conference on Robotics and Automation (ICRA)*, 2022, pp. 5162–5169.
- [16] C. Pogue, P. Rao, Q. Peyron, J. Kim, J. Burgner-Kahrs, and E. Diller, "Multiple Curvatures in a Tendon-Driven Continuum Robot Using a Novel Magnetic Locking Mechanism," in *IEEE International Conference on Intelligent Robots and Systems*, vol. 2022-October. Institute of Electrical and Electronics Engineers Inc., 2022, pp. 472–479.
- [17] R. Zhao, H. Dai, and H. Yao, "Liquid-metal magnetic soft robot with reprogrammable magnetization and stiffness," *IEEE Robotics and Automation Letters*, vol. 7, no. 2, pp. 4535–4541, 2022.
- [18] R. Baines, S. K. Patiballa, J. Booth, L. Ramirez, T. Sipple, A. Garcia, F. Fish, and R. Kramer-Bottiglio, "Multi-environment robotic transitions through adaptive morphogenesis," *Nature (London)*, vol. 610, no. 7931, pp. 283–289, 2022.
- [19] J. Zhang, B. Wang, H. Chen, J. Bai, Z. Wu, J. Liu, H. Peng, and J. Wu, "Bioinspired Continuum Robots with Programmable Stiffness by Harnessing Phase Change Materials," *Advanced materials technologies*, vol. 8, no. 6, pp. 2201616-n/a, 2023.
- [20] Y. Kim, S. S. Cheng, and J. P. Desai, "Active stiffness tuning of a spring-based continuum robot for mri-guided neurosurgery," *IEEE Transactions on Robotics*, vol. 34, no. 1, pp. 18–28, 2018.
- [21] M. Mirkhalaf and A. Rafsanjani, "Harnessing machine mechanisms to continuously reprogram metamaterials," *Matter*, vol. 6, 2023.
- [22] J. Burgner-Kahrs, D. C. Rucker, and H. Choset, "Continuum Robots for Medical Applications: A Survey," *IEEE transactions on robotics*, vol. 31, no. 6, pp. 1261–1280, 2015.
- [23] A. Leavitt, R. Lam, Nichols Crawford Taylor, D. S. Drew, and A. Kuntz, "Toward a Millimeter-Scale Tendon-Driven Continuum Wrist with Integrated Gripper for Microsurgical Applications," *arXiv.org*, 2023.
- [24] T. Wang, H. Li, T. Pu, and L. Yang, "Microsurgery robots: Applications, design, and development," *Sensors*, vol. 23, no. 20, 2023.